URSI GASS 2020, Rome, Italy, 29 August - 5 September 2020

Characterization of Indoor Environment in the 60 GHz band

Amar Al-jzari, Jack Towers, and Sana Salous*
Department of Engineering, Durham University, Durham, DH1 3LE UK, * sana.salous@durham.ac.uk

Abstract

The millimeter-wave (mmWave) band will be used for the fifth generation (5G) wireless communication systems. In this paper, results of wideband channel measurements conducted at Durham University campus in various indoor environments are presented. The measurements were performed with 6 GHz bandwidth (BW) in the V-band using a multiband chirp-based channel sounder. The multipath component parameters (MPCs) including power delay profile (PDP), power angle profile (PAP), root mean square (RMS) delay spread (DS), and angular spread (AS) have been estimated and compared in order to characterize the measured channel. The results will be valuable for future mmWave communication systems design in indoor environments.

1 Introduction

The overwhelming demand for broadband wireless communications has prompted the wireless industry, academics, and regulators to consider scaling up to the mmWave spectrum. This would be used primarily for 5G wireless communication systems where a vast amount of raw bandwidth will provide multi-gigabit-per-second (Gbps) data rate transmission throughputs [1, 2]. Whilst mmWave communication offers high data rates, it will have widely different propagation channel characteristics compared with sub-6 GHz frequency bands such as high propagation loss and susceptibility to shadowing (e.g. blockage by humans or obstacles) [3]. These impairments can be mitigated by employing high gain beam steerable antenna arrays.

The focus of this research is the 60 GHz band for short-range indoor communications, due to the availability of 5-7 GHz of unlicensed bandwidth [4, 5]. This has motivated different 60 GHz indoor propagation measurements to provide a comprehensive and accurate understanding of the radio propagation channel characteristics, which is essential for successful development and optimal deployment of future wireless networks. Various channel measurement campaigns have been performed in the 60 GHz band in different indoor scenarios, in order to study the radio propagation channel characteristics [3]-[8]. The measured scenarios include an office, corridor, hall and laboratory as well as many others. The measurement results provide large-scale channel parameters and small-scale fading channel parameters. In this paper, wideband indoor channel measurements where conducted in the 60 GHz ISM band in a meeting room, a classroom and a computer laboratory to measure and estimate different relative channel parameters. The measurements were performed using the multiband Frequency Modulated Continuous Wave (FMCW) channel sounder developed at Durham University [7]-[10].

The rest of the paper is organized as follows. Section 2 describes the measurement scenarios and measurement system setup. Section 3 outlines the channel parameters to be estimated. Section 4 covers the associated results of these measurements. Concluding remarks will then be given in Section 5.

2 Measurement Set-up and Scenarios

The indoor propagation measurement campaigns were performed in the V-band in the frequency range of (59.6 - 65.6 GHz) with a sweep rate of 1.22 kHz. In each measured scenario, the transmitter (Tx) location was placed at the corner while the receiver (Rx) was moved onto predefined locations within the scenario. The Tx and Rx were also set at different height to emulate typical WLAN network environment. To investigate the angular variation of the wideband channel, the RF heads were mounted onto a CCTV positioner to rotate the directional antennas. Hence, for measuring Angle of Departure (AoD), the Rx unit was fixed while the Tx was rotated with a step size of 15 degrees in the azimuth plane to cover the full rotation. Therefore, 24 data files were recorded at each location corresponding to the full 360-degree azimuthal coverage. At each angular rotation the data were recoded for two seconds duration with 40 MHz sampling rate ADC. Table 1 gives a summary of the conducted channel measurement set-up parameters for each measured scenario. Figure 1 shows pictures of some of the measured environments. In each scenario between 9 and 16 Rx locations were measured.

Table 1. Sounder unit set-up parameters.

System Parameters	
Frequency Range (GHz)	59.6-65.6
Sweep Rate (kHz)	1.22
Sampling Rate (MHz)	40
Link Polarization	V-V
Tx Antenna (gain, beam)	20 dBi, Horn (~18º)
Rx Antenna	Omni-directional
Tx (Rx) Antenna Height (m)	2.5-2.8 (1)

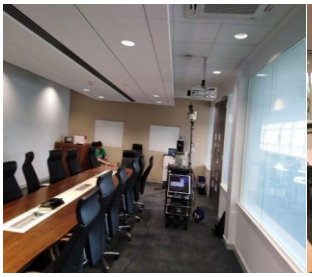

(a) Meeting room

(b) Classroom

(c) Computer Lab.

Figure 1. Indoor measurement environments.

3 Estimated Channel Parameters

The raw data were analyzed for 0.5 ns time delay resolution equivalent to 2 GHz BW in order to estimate different relative channel parameters. These parameters were estimated from the channel Power Delay Profile (PDP) given in equation (1), which is the average of the channel impulse response (CIR) $h_k(t_k,\tau)$ obtained over 2 second (s) for each angle of rotation of the Tx or the Rx.

$$PDP(\tau) = P(\tau) = \sum_{k=1}^{K} |h_k(t_k,\tau)|^2 \,/K \qquad (1)$$

where (τ) is the time delay, K is the total number of the CIR snapshots obtained in each angle direction within 2s. Prior to extracting the relevant channel parameters, the noise floor is calculated in each PDP and a threshold is set above it in order to remove the noise samples from the PDP. The received power angle profile ($P_R(\emptyset_i)$), at each azimuth angle ($\emptyset_i$), is shown in equation (2) as the sum of the corresponding noise free PDP [7]-[10].

$$P_R(\emptyset_i) = \sum_{n=1}^{N} P(\tau_n, \emptyset_i) \qquad (2)$$

where τ_n is the excess delay of the n^{th} tap delay and N is the number of delay bins in each PDP. $\emptyset_i$ is restricted to the range of +/- π.

The channel RMS Delay spread (RMS DS) is used to characterize the time dispersion properties of wideband channels due to multipath. The RMS DS was estimated using equation (3) [7]-[10].

$$\tau_{rms} = \sqrt{\frac{\sum_{n=1}^{N}(\tau_n - \tau_m)^2\, P\,(\tau_n)}{\sum_{n=1}^{N} P\,(\tau_n)}} \qquad (3)$$

where $P(\tau_n)$ is the received power at delay τ_n and τ_m is the mean delay spread and can be expressed as in equation (4).

$$\tau_m = \frac{\sum_{n=1}^{N} P\,(\tau_n)\ \tau_n}{\sum_{n=1}^{N} P\,(\tau_n)} \qquad (4)$$

The Angular Spread (AS) of the channel is used to characterize the directional distribution of the departing or arriving energy. The mean azimuth Angle of Departure (AoD) or Arrival (AoA) was estimated using equation (5).

$$\emptyset_m = \arg\left(\frac{\sum_{i=1}^{L} P_R(\emptyset_i)\, e^{i\emptyset_i}}{\sum_{i=1}^{L} P_R(\emptyset_i)}\right) \qquad (5)$$

where $\emptyset_m$ is the mean azimuthal angle of arrival or departure and L is the total number of each angle position. The mean azimuth angle is then used to obtain the angular spread ($\emptyset_{AS}$) that will be estimated from the corresponding received Power Angle Profile (PAP) using equation (6) [7]-[10].

$$\emptyset_{AS} = \sqrt{\frac{\sum_{i=1}^{L} P_R(\emptyset_i)\,((\emptyset_i - \emptyset_m)^2)}{\sum_{i=1}^{L} P_R(\emptyset_i)}} \qquad (6)$$

4 Results and Analysis

4.1 Power Delay Profile (PDP)

The PDP is an important channel parameter that shows the received signal power distribution over different time delays as shown in Fig. 2. It displays an example of the relative PDP at one location in the meeting room environment, versus the rotation angle at the Tx side, where the PDP normalized to the maximum received signal level over all PDPs. The strong, main component can be observed at around – 65° corresponding to the boresight (BS) angle when the Tx and Rx antennas are pointing to each other. Another peak appears at around 70° and -130° when the Tx antenna is orientated to the opposite direction and these multipath reflections caused by reflections from the glass wall and the concrete walls. Figure 3 shows the PDP of the BS (LOS) angle when the Tx and Rx antenna main beams are aligned in the absence of the obstruction as well as the PDP of the obstructed LOS (OLOS) angle (non-boresight (NBS) angle) when the main beams are not aligned or an obstruction existed between the Tx and Rx. The strongest received power, corresponding to LOS, can be observed when the Tx is aligned with BS, while the power is reduced when the antennas are misaligned (NBS).

4.2 Power Angle Profile (PAP)

The PAP represents the received power at each angle. Figure 4 depicts an example of the computed PAP at one location in the meeting room scenario. The highest power value is achieved at the BS angle which represents the LOS path. The two other peak power values represent OLOS paths occurring due to reflections within the room.

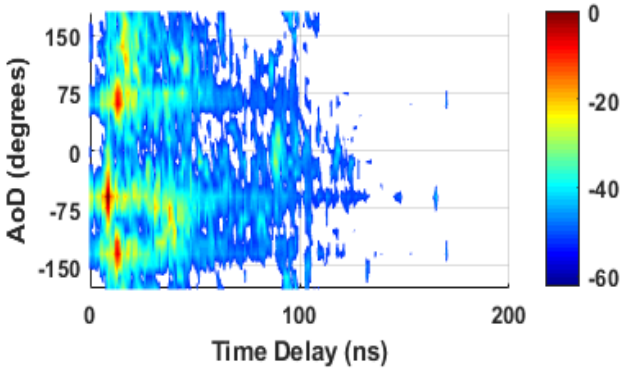

Figure 2. Relative power delay profile vs. azimuth angle of rotation in the meeting room environment.

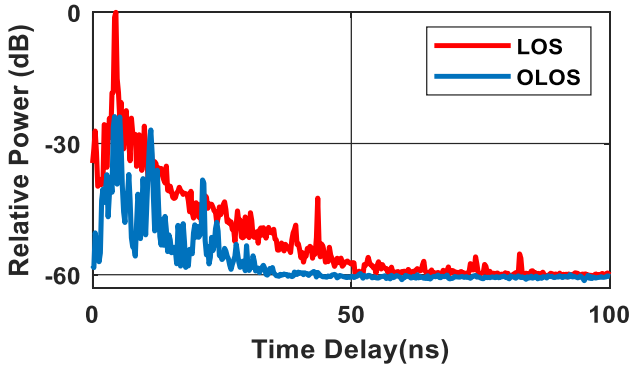

Figure 3. Relative power delay profile for LOS and OLOS angles in the meeting room environment.

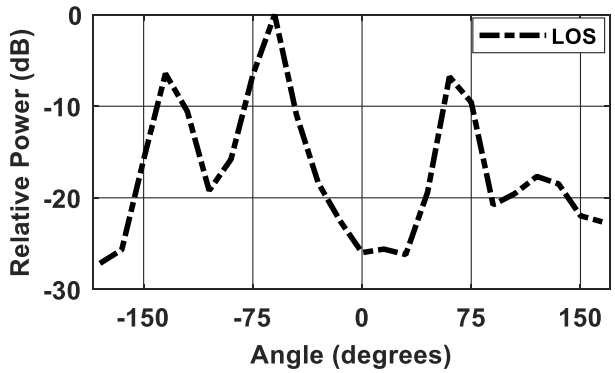

Figure 4. Received power as function of rotation angle in the meeting room environment.

4.3 Delay Spread (RMS DS)

Figure 5. shows the cumulative distribution function (CDF) of the RMS DS values for the meeting room scenario. During the processing, the RMS DS of each measured position was estimated for a 20 dB threshold from the peak in each PDP and categorized based on the relative angular direction between the Tx and Rx antennas into BS (LOS) and NBS (OLOS). Table 2 is a summary of the τ_{rms} values in ns at CDF level of 50% and 95% as well as the corresponding standard deviation, for each scenario. In all measured environments, the LOS senario has smaller RMS DS values than OLOS senario due to less obstrutions and multipath components. Figure 6 displays the RMS DS as a function of Tx-Rx separation distance, indicating the mean value across all the distance is approximately 6 ns.

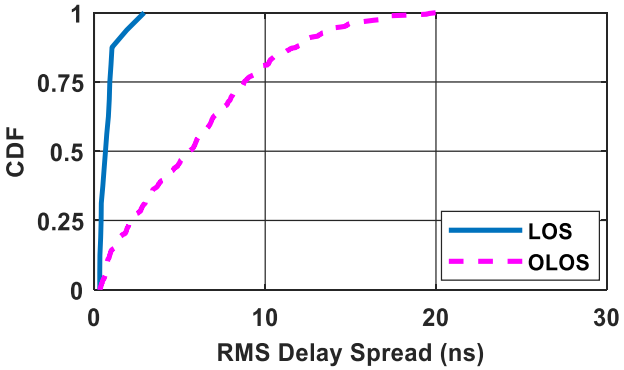

Figure 5. CDF of the RMS DS values for the meeting room environment.

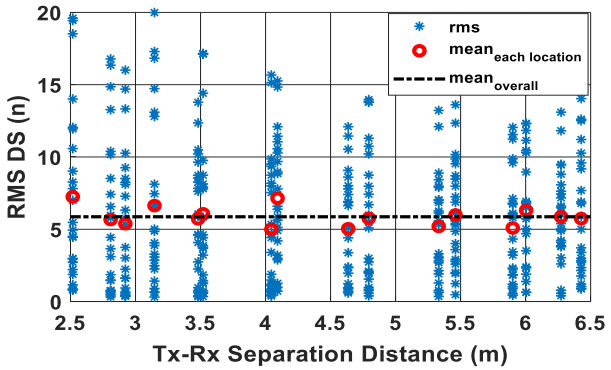

Figure 6. RMS DS values as a function of Tx-Rx separation distance.

Table 2. Summary of RMS DS values for each scenario.

Delay Spread Statistic CDF = 50 %; CDF = 95%; $\sigma_{\tau_{rms}}$		
Scenario	**LOS (BS)**	**OLOS (NBS)**
Meeting Room	0.65; 2.09; 0.68	5.58; 14.59; 6.33
Computer Lab.	2.20; 10.22; 3.78	11.30; 21.90; 6.34
Classroom	2.68; 10.11; 3.59	13.81; 26.58; 6.92

4.4 Angular Spread (AS)

The CDF of the AS ($\emptyset_{AS}$) values for the three measured environments was computed and a summary is given in Table 3 in degrees for the 50% and 95% values as well as the corresponding standard deviation, for each scenario. The results indicate the meeting room, which is the smallest in area, exhibited a smaller AS which could be attributed to less reflectors and scatterers with respect to the other two environments where there were more likely to be reflected paths from glass and walls. The AS value vs. Tx-Rx separation distance, shown in Figure 7, indicates a decreasing AS the Tx-Rx separation increased.

Table 3. Summary of AS values for each scenario.

Angular Spread Statistic *CDF = 50 %; CDF = 95%; $\sigma_{\emptyset_{AS}}$*	
Scenario	**LOS**
Meeting Room	109.59; 127.71; 7.89
Computer Lab.	153.23; 189.38; 26.44
Classroom	122.87; 135.34; 10.70

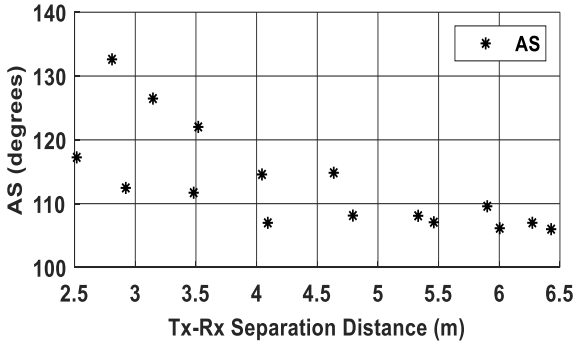

Figure 7. AS values as a function of Tx-Rx separation distance.

5 Conclusion

A wideband FMCW channel sounder was used to perform mmWave channel measurements in various indoor scenarios to study the radio propagation channel characteristics in the 60 GHz band. The parameters that are used to characterize the spatial and temporal variation of the wideband channel were estimated from the present measurements. It was observed that when the antennas become misaligned, OLOS, the rms time delay spread more than doubles for both the 50% and 95% CDF values. Furthermore, the AS values emphasize the fact that indoor environments are multipath rich and therefore have larger angular spread values than outdoor environments [9].

6 Acknowledgements

The authors would like to acknowledge the support of WaveComBE project, under Horizon 2020 research and innovation program, grant agreement No. 766231 and Intel USA. The 60 GHz sounder was developed under the EPSRC grant PATRICIAN EP/I00923X/1.

7 References

1. Rangan, S., Rappaport, T., Erkip, E., "Millimeter wave cellular wireless networks: potentials and challenges," IEEE Proc., 2014, 102, (3), pp. 366-385.

2. G. R. Maccartney, T. S. Rappaport, S. Sun and S. Deng, "Indoor Office Wideband Millimeter-Wave Propagation Measurements and Channel Models at 28 and 73 GHz for Ultra-Dense 5G Wireless Networks," in *IEEE Access*, vol. 3, pp. 2388-2424, 2015.

3. X. Wu *et al*., "60-GHz Millimeter-Wave Channel Measurements and Modeling for Indoor Office Environments," in *IEEE Transactions on Antennas and Propagation*, vol. 65, no. 4, pp. 1912-1924, April 2017.

4. K. Haneda, J. Järveläinen, A. Karttunen, M. Kyrö and J. Putkonen, "Indoor short-range radio propagation measurements at 60 and 70 GHz," *The 8th European Conference on Antennas and Propagation (EuCAP 2014)*, The Hague, 2014, pp. 634-638.

5. A. Maltsev *et al*., "Characteristics of indoor millimeter-wave channel at 60 GHz in application to perspective WLAN system," *Proceedings of the Fourth European Conference on Antennas and Propagation*, Barcelona, 2010, pp. 1-5.

6. Hao Xu, V. Kukshya and T. S. Rappaport, "Spatial and temporal characteristics of 60-GHz indoor channels," in *IEEE Journal on Selected Areas in Communications*, vol. 20, no. 3, pp. 620-630, April 2002.

7. S. Salous, S. M. Feeney, X. Raimundo and A. A. Cheema, "Wideband MIMO Channel Sounder for Radio Measurements in the 60 GHz Band," in *IEEE Transactions on Wireless Communications*, vol. 15, no. 4, pp. 2825-2832, April 2016.

8. X. Raimundo, S. Salous and A. A. Cheema, "Indoor radio propagation measurements in the V-band," *Radio Propagation and Technologies for 5G (2016)*, Durham, 2016, pp. 1-5.

9. X. Raimundo, S. El-Faitori, Y. Cao and S. Salous, "Outdoor directional radio propagation measurements in the V-band," *2018 IEEE 29th Annual International Symposium on Personal, Indoor and Mobile Radio Communications (PIMRC)*, Bologna, 2018, pp. 790-794.

10. X. Raimundo, S. Salous and A. Cheema, "Indoor dual polarised radio channel characterisation in the 54 and 70 GHz bands," in *IET Microwaves, Antennas & Propagation*, vol. 12, no. 8, pp. 1287-1292, 4 7 2018.